Uniaxial Shear-Flexure Model for Reinforced Concrete Elements

H. Mostafaei[1] and F. J. Vecchio[2]

Abstract: A simple approach was developed for performance-based analysis of reinforced concrete columns subjected to shear, flexure and axial loads. This method is based on a simplification of a consistent but relatively more complex approach known as the axial-shear-flexure interaction (ASFI) method, which is able to predict the full load-deformation relationships of reinforced concrete columns subjected to axial, flexure and shear force. The uniaxial shear-flexure model (USFM), presented herein, can also predict comparable full load-deformation responses. In it, however, the computation-intensive iteration process for shear modeling used within the ASFI approach is eliminated and the formulation is simplified. This paper describes the formulation, implementation and verification of the USFM approach.

DOI: 10.1061/(ASCE)0733-9445(2008)134:9(1538)

CE Database subject headings: Beams; Columns; Nonlinear analysis; Flexural strength; Axial forces; Deformation; Performance characteristics; Reinforced concrete.

Introduction

Among the most common analytical methods for displacement-based analysis of reinforced concrete columns and beams are the section analysis method and the uniaxial fiber model, both developed based on the same concept. In both approaches, a reinforced concrete column or beam is discretized and analyzed by employing uniaxial elements and ignoring the shear response. However, the performance of reinforced concrete elements dominated in shear or shear-flexure cannot be estimated by either fiber modeling or section analysis, since the shear behavior is not taken into account in either of these approaches. Recently, an attempt was made to include the effects of shear deformations in sectional analyses through the axial-shear-flexure interaction (ASFI) method by (Mostafaei and Kabeyasawa 2005, 2007).

The ASFI method was developed to improve not only the response simulation of reinforced concrete elements with dominant shear behavior, but also to modify the flexural response of the fiber model approach. This was done by satisfying the compatibility and equilibrium conditions for both the flexure and shear mechanisms employed in the ASFI method. In the approach, the flexure mechanism was modeled by applying traditional section analysis techniques, and shear behavior was modeled based on the modified compression field theory (MCFT), developed by Vecchio and Collins (1986). The approach was implemented and verified for a number of reinforced concrete columns tested with different axial loads, transverse reinforcement ratios, longitudinal reinforcement ratios, and scales ranging from one-third to full-scale specimens. However, the application of the MCFT, as a shear model within the ASFI method, requires a relatively intensive computation and iteration process, which might not be amenable to engineers for routine practice.

In this study, an attempt is made to simplify the shear behavior modeling of the axial-shear-flexure interaction approach into a uniaxial analytical concept. In the uniaxial-shear-flexure model (USFM) approach, the axial strain and principal tensile strain of a reinforced concrete column or beam, between two adjoining flexural sections, are determined based on the average axial strains and average resultant concrete compression strains of the two sections. This simplifies the approach significantly by eliminating the iteration process for the shear model of the ASFI method.

Verification of the model's accuracy is also provided by examining data from several series of reinforced concrete columns test specimens, demonstrating results comparable with the original ASFI method. An Excel program file for the USFM can be acquired via a contact with the first author.

Background to ASFI Method

The ASFI method is comprised of two models: a flexure model based on traditional uniaxial section analysis, and a shear model based on a biaxial shear element approach. The total lateral drift of the column between two sections γ is taken as the sum of shear strain (γ_s) and the flexural drift ratio (γ_f) between the two sections. Furthermore, the total axial strain of the column between the two sections ε_x is taken as the sum of axial strains due to axial (ε_{xa}), shear (ε_{xs}), and flexural (ε_{xf}) mechanisms

$$\gamma = \gamma_s + \gamma_f \tag{1a}$$

$$\varepsilon_x = \varepsilon_{xs} + \varepsilon_{xf} + \varepsilon_{xa} \tag{1b}$$

The centroidal strain ε_{xc} is derived from a section analysis, or an axial-flexure model, and is defined as the sum of the strains

[1]Postdoctoral Fellow, Dept. of Civil Engineering, Univ. of Toronto, ON, Canada, M5S 1A4.

[2]Professor, Dept. of Civil Engineering, Univ. of Toronto, ON, Canada, M5S 1A4.

Note. Associate Editor: Dat Duthinh. Discussion open until February 1, 2009. Separate discussions must be submitted for individual papers. The manuscript for this paper was submitted for review and possible publication on June 5, 2007; approved on February 1, 2008. This paper is part of the ***Journal of Structural Engineering***, Vol. 134, No. 9, September 1, 2008. ©ASCE, ISSN 0733-9445/2008/9-1538–1547/ $25.00.

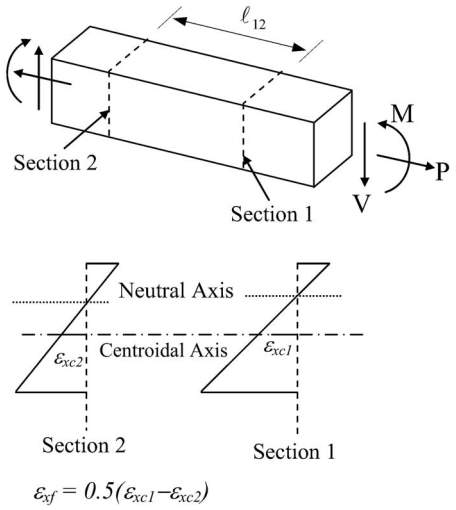

Fig. 1. Average centroidal strain due to flexure

due to axial and flexural mechanisms $\varepsilon_{xc}=\varepsilon_{xaf}+\varepsilon_{xf}$. On the other hand, from the shear model or from an axial-shear element, the sum of the strains due to axial and shear mechanisms is determined, $\varepsilon_s=\varepsilon_{xas}+\varepsilon_{xs}$. As a result, to obtain ε_x in Eq. (1*b*), ε_{xf} must be extracted from ε_{xc} (Fig. 1) and added to ε_s, assuming $\varepsilon_{xa}=\varepsilon_{xaf}=\varepsilon_{xas}$.

Equilibrium of the shear and axial stresses from the axial-flexure element τ_f and σ_{xf} and from the axial-shear model τ_s and σ_{xs}, respectively, must be satisfied simultaneously through the analysis. That is

$$\sigma_{xf}=\sigma_{xs}=\sigma_o \quad \tau_f=\tau_s=\tau \tag{2}$$

where σ_{xf}=axial stress in axial-flexure mechanism; σ_{xs}=axial stress in axial-shear mechanism; σ_o=applied axial stress; τ_f=shear stress in axial-flexure mechanism; τ_s=shear stress in axial-shear mechanism; and τ=applied shear stress. Stresses in axes perpendicular to the axial axis of the column, the clamping stresses σ_y and σ_z, are ignored due to equilibrium between confinement pressure and hoops stresses

$$\sigma_y=\sigma_z=0 \tag{3}$$

Fig. 2 illustrates the two models for axial shear and axial flexure, and their interactions, by means of springs in series. Fig. 3 illustrates the ASFI method, for a reinforced concrete column with two end sections, including the equilibrium and compatibility conditions. The total axial deformations considered in the ASFI method are axial strains developed by axial, shear, and flexure, and by pullout mechanisms. The total drift ratio is a combination of shear, flexure, and pullout deformations as shown in Fig. 4. In the ASFI method, the pullout components of rotation and slip are determined based on the model developed by Okamura and Maekawa (1991).

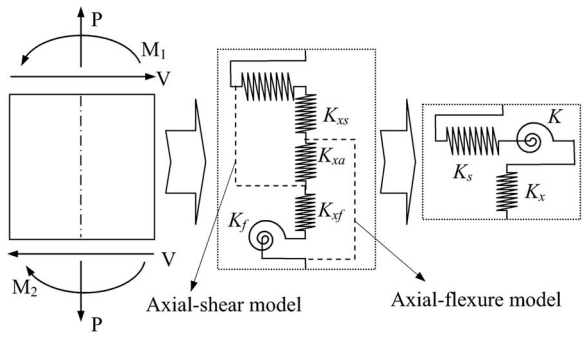

Fig. 2. Springs model of ASFI method

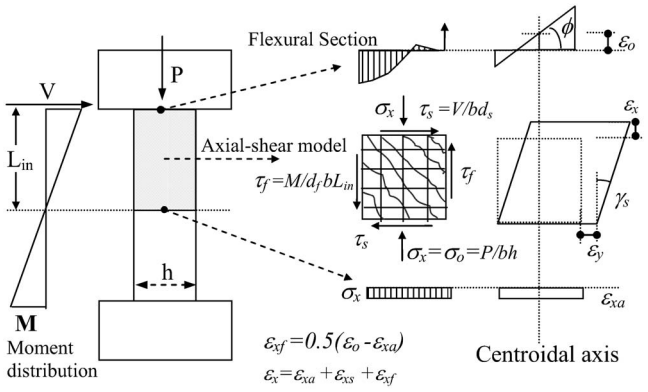

Fig. 3. Axial-shear-flexure interactions in ASFI method

Conceptual Model

Consider a beam subjected to a bending moment, with the strain and stress relationships at a flexural section as shown in Fig. 5. The main treatment on the section analysis implemented in the USFM is to employ a compression softening factor, β, obtained based on the MCFT for an element between two adjacent sections, one of which would be the section represented in Fig. 5. The compression softening factor is applied to the concrete compression stress to represent degradation in the concrete strength due to shear deformation. In addition to the compression softening factor, the shear stress at crack locations is determined and checked. If the equilibrium at a shear crack gives shear stress less than the shear stress obtained from section analysis, the lower shear stress at crack is considered as the shear stress acting on the element.

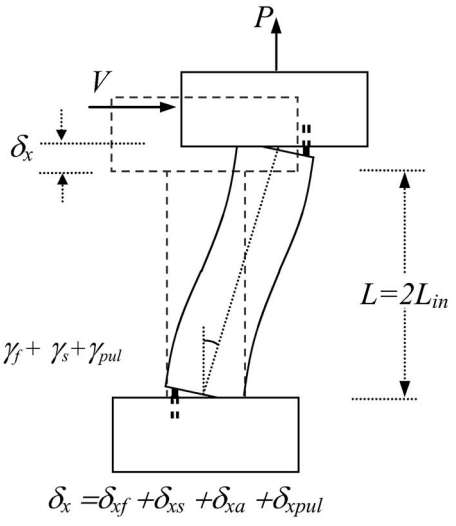

Fig. 4. Axial and shear deformations of a column considered by ASFI method

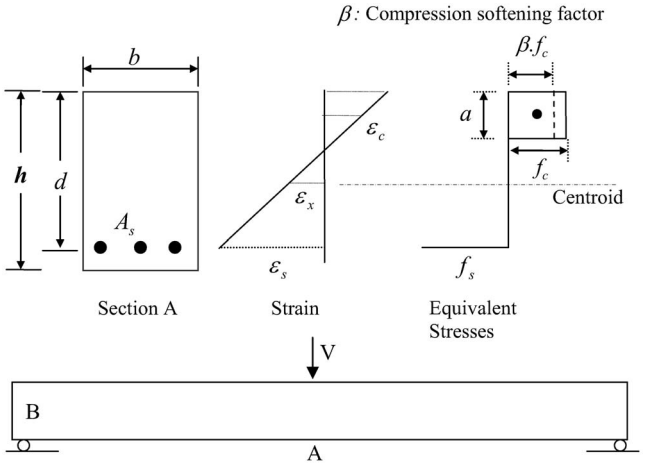

Fig. 5. Stress-strain relationships at a flexural section

To obtain the compression softening factor, at least two flexural sections must be defined along the element. For the beam example in Fig. 5, given the symmetric conditions, Sections A and B can be taken as the two flexure sections required. Since the moment is zero at Section B, typically, Section A is the main flexure section used for the analysis. The compression softening factor is determined based on the average concrete tensile strain ε_1 of the element between Sections A and B, calculated according to Eq. (4)

$$\beta = \frac{1}{0.8 - 0.34\dfrac{\varepsilon_1}{\varepsilon_c'}} \leq 1.0 \tag{4}$$

where ε_c'=concrete strain at the cylinder peak uniaxial compressive stress. The average concrete tensile strain ε_1 is determined according to two basic assumptions and the fundamental equation of the MCFT, as described in the following sections.

Basic Assumptions

Consider a reinforced concrete column, fixed against rotation and translation at the bottom and free at the top, subjected to in-plane lateral load and axial load as shown in Fig. 6. Given its pattern along the column [see Fig. 6(a)], the concrete principal compression strain for an element between two sections ε_2 might be determined based on the average value of concrete uniaxial compression strains corresponding to the resultant forces of the concrete stress blocks. That is

$$\varepsilon_2 = 0.5(\varepsilon_{2_i} + \varepsilon_{2_{i+1}}) \tag{5}$$

Eq. (5) represents the first main hypothesis of the USFM method. This assumption simplifies the shear model significantly from a biaxial to a uniaxial mechanism. For the column in Fig. 6, the compression strain obtained from the above equation is set equal to the average principal compression strain of the element between the two sections of i and $i+1$.

This assumption is applicable as long as the concrete compression stress within the stress block, due to moment and axial load, is larger than the shear stress applied to the section. Accordingly, the principal stress for a small element within the domain can be calculated as

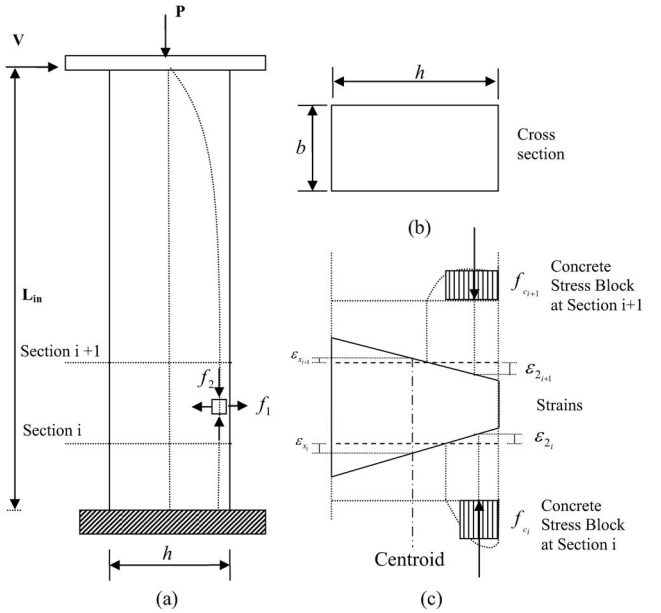

Fig. 6. Reinforced concrete column subjected to shear and axial loads; (a) concrete principal compression stress pattern; (b) cross section; and (c) stress blocks and strains at two subsequent sections

$$f_2 = 0.5(f_x + f_y) + \sqrt{0.25(f_x - f_y)^2 + \tau^2} \tag{6}$$

For any point next to the concrete stress block, considering f_y sufficiently small to be negligible and setting $f_x = f_c$, where f_c=concrete compression stress from the stress block, Eq. (6) can be simplified to

$$f_2 = 0.5f_c + \sqrt{0.25f_c^2 + \tau^2} \tag{7}$$

where $\tau = V/bh$. For the element in Fig. 6 but with $P=0$, by ignoring compression bar stresses, $M = VL_{in} = f_c abd_v$, hence

$$f_c = \frac{VL_{in}}{abd_v} \tag{8}$$

where a=equivalent width of the stress block and d_v=lever arm. As an example, for a short beam with shear span-to-depth ratio of 1, $L_{in}=h$, with an approximate value of $0.7h$ for d_v and $0.3h$ for a, hypothetically

$$f_c = 4.8\frac{V}{bh} = 4.8\tau \Rightarrow \tau = 0.21f_c$$

As the result: $f_2 = 0.5f_c + \sqrt{0.25f_c^2 + (0.21f_c)^2} = 1.04f_c$.

Hence, for a short beam with conventional loading conditions, the effect of shear stress on the principal compression stress is minor. In general, L is typically much greater than h and the difference between shear stress (τ) and stress block compressive stress (f_c) decreases to a negligible value. This difference is smaller in the case of columns under compression, since the axial load increases the axial normal stress. On the other hand, if an element is subjected to pure shear stress, such as with shear panels, or to relatively small normal stress, such as shear walls, L may be less than h and this assumption needs to be reconsidered.

A second main assumption of the USFM is the definition of the average axial strain at the centroid, obtained by averaging the values of the axial strains at the two sections

$$\varepsilon_x = 0.5(\varepsilon_{x_{i_i}} + \varepsilon_{x_{i+1}}) \tag{9}$$

The normal strain due to shear stress in the axial direction could be determined using the MCFT and added to the above equation. However, it will be shown later that this would not have a significant effect, in many cases, on responses obtained by the USFM.

These two assumptions, namely, Eqs. (5) and (9), enable a simplification of the MCFT. Now, the concrete principal tensile strain can be determined as described in the following section.

Concrete Principal Tensile Strain

To determine the compression softening factor β using Eq. (4), the main challenge is to obtain the concrete principal tensile strain ε_1. This requires application of the modified compression field theory for the element between the two adjacent flexural sections in Fig. 6(c). From the MCFT, equilibrium conditions require that

$$f_{cx} = f_{c1} - \tau \cot \theta \tag{10}$$

$$f_{cy} = f_{c1} - \tau \tan \theta \tag{11}$$

where f_{cx} and f_{cy}=stresses in concrete in the x (axial) and y (transverse) directions, respectively; f_{c1}=concrete principal tensile stress; τ=concrete shear stress; and θ=crack angle. Using the equilibrium equations [Eqs. (10) and (11)] the following relationship can be derived:

$$\tan^2 \theta = \frac{f_{c1} - f_{cy}}{f_{c1} - f_{cx}} \tag{12}$$

On the other hand, the compatibility condition of the MCFT requires that

$$\tan^2 \theta = \frac{\varepsilon_x - \varepsilon_2}{\varepsilon_y - \varepsilon_2} \tag{13}$$

where ε_x=axial strain; ε_y=strain of transverse reinforcement; and ε_2=concrete principal compression strain. Extracting θ from Eqs. (12) and (13) gives the following equation independent from the crack angle θ:

$$\frac{f_{c1} - f_{cy}}{f_{c1} - f_{cx}} = \frac{\varepsilon_x - \varepsilon_2}{\varepsilon_y - \varepsilon_2} \tag{14}$$

This is the main equation employed by the USFM to determine ε_y, which is then used to calculate ε_1 as follows:

$$\varepsilon_1 = \varepsilon_x + \varepsilon_y - \varepsilon_2 \tag{15}$$

Eq. (14) is solved for ε_y considering two cases: first, for the case where the strain in the transverse reinforcement is less than the yield strain and, second, for the case where the transverse bars have yielded.

Case I

When strain in the transverse reinforcement ε_y is less than the yield strain, $\varepsilon_y \leq \varepsilon_{yy}$. From the equilibrium condition of the MCFT

$$f_y = f_{cy} + \rho_{sy} f_{sy} \tag{16}$$

where f_y=total normal or clamping stress in y direction, taken to be zero; f_{cy}=concrete stress in the y direction; ρ_{sy}=transverse reinforcement ratio; and f_{sy}=stress in transverse reinforcement. Therefore, by considering a linear stress-strain relationship for transverse reinforcements $f_{sy}=E_s\varepsilon_y$, Eq. (16) is simplified as

$$f_{cy} = -\rho_{sy} E_s \varepsilon_y \tag{17}$$

where ε_y=strain in the transverse reinforcement; and E_s=modulus of elasticity of the transverse reinforcement.

Substituting Eq. (17) into Eq. (14) and solving for ε_y gives

$$\varepsilon_y = \sqrt{b^2 + c} - b \tag{18}$$

where

$$b = \frac{f_{c1}}{2\rho_{sy} E_s} - \frac{\varepsilon_2}{2}$$

$$c = \frac{(\varepsilon_x - \varepsilon_2)(f_{c1} - f_{cx}) + f_{c1}\varepsilon_2}{\rho_{sy} E_s}$$

and

$$f_{cx} = f_x - \rho_{sx} f_{sx}$$

where f_x=applied axial load; f_{sx}=stress in the x direction reinforcement (i.e., the longitudinal bar stress) obtained from the section analysis based on the average centroidal strain; ε_x and ε_2=normal and concrete principal compression strains determined from the two main assumptions of the USFM [i.e., Eqs. (5) and (9)]; and f_1=concrete principal tensile stress.

In the USFM, the shear mechanism has no effect on the sectional analysis up to when $\beta \leq 1$ or, from Eq. (4) with $\varepsilon_c' = -0.002$, $\varepsilon_1 \geq 0.0012$. Hence, the concrete tensile stress might be limited as

$$f_{c1} = \frac{f_t'}{1 + \sqrt{500\varepsilon_1}} \leq 0.56 f_t' \text{ for } \beta \leq 1 \tag{19}$$

Applying a minimum concrete compression strength of $0.2f_c'$, the lower bounds for β and f_{c1} are 0.2 and $0.31f_t'$, respectively; hence

$$0.56 f_t' \geq f_{c1} \geq 0.31 f_t' \tag{20}$$

If an iteration process is implemented for the section analysis, typically, an initial value of $0.56f_t'$ might be employed for f_{c1}. For each iteration, then f_{c1}, can be recalculated based on the ε_1 obtained in the previous iteration. However, using an average value of $f_{c1}=0.44f_t'$ would give a reasonably accurate average compression softening factor β for the specimens, avoiding any iteration for solving Eq. (18).

Another consideration would be the normal strain in the x direction due to shear stress, which is included in the calculation of ε_x in Eq. (9). Comparing Eqs. (9) and (1) reveals that Eq. (9) contains only the normal strains due to the flexure and axial mechanisms and not that of the shear mechanism ε_{xs}. The shear component of the axial strain ε_{xs} can be determined based on the MCFT and added to the ε_x in Eq. (9)

$$\varepsilon_{xs} = \frac{\tau \cot \theta - f_{c1}}{E_s \rho_{sx}} \geq 0 \tag{21}$$

where $E_s\rho_{sx} \leq f_{sxy}$, and where f_{sxy}=yield stress of the longitudinal bars.

Hence

$$\varepsilon_x = 0.5(\varepsilon_{x_{i_i}} + \varepsilon_{x_{i+1_i}}) + \varepsilon_{xs} \tag{22}$$

The shear component of the normal strain in the x direction, for conventional beams and columns where the flexural deformations are larger than the shear deformations, can generally be

Table 1. Material Property of the Specimens

Specimen	Type	b mm (in.)	h mm (in.)	$2L_{in}$ mm (in.)	S_h mm (in.)	ρ_g %	ρ_w %	f_{yx} MPa (ksi)	f_{yy} MPa (ksi)	$f'c$ MPa (ksi)	P kN (kips)
No. 12	DC	300 (11.8)	300 (11.8)	900 (35.4)	150 (5.9)	2.26	0.14	415 (60)	410 (59)	28 (4.1)	540 (121.3)
No. 14	DC	300 (11.8)	300 (11.8)	900 (35.4)	50 (2.0)	2.26	0.43	415 (60)	410 (59)	26 (3.8)	540 (121.3)
No. 15	DC	300 (11.8)	300 (11.8)	900 (35.4)	50 (2.0)	2.26	0.85	415 (60)	410 (59)	26 (3.8)	540 (121.3)
No. 16	DC	300 (11.8)	300 (11.8)	600 (23.6)	50 (2.0)	1.8	0.43	415 (60)	410 (59)	27 (3.9)	540 (121.3)
RCF-L	DC	250 (9.8)	250 (9.8)	1,400 (55.1)	100 (3.9)	1.82	0.1	390 (57)	325 (47)	20 (2.9)	Varying 125←300 (28)←(67)
RCF-R	DC	250 (9.8)	250 (9.8)	1,400 (55.1)	100 (3.9)	1.82	0.1	390 (57)	325 (47)	20 (2.9)	Varying 300→475 (67)←(107)
A1	DC	150 (5.9)	420 (16.5)	1,260 (49.6)	200 (7.9)	0.9	0.13	350 (51)	290 (42)	18.3 (2.7)	328 (74)
B1	DC	300 (11.8)	300 (11.8)	900 (35.4)	160 (6.3)	1.69	0.08	336 (49)	290 (42)	18.3 (2.7)	477 (107)
U6	SC	350 (13.8)	350 (13.8)	2,000 (78.7)	65 (2.6)	3.2	0.85	437 (63)	425 (62)	37.3 (5.4)	600 (135)
2CLH18	DC	457 (18)	457 (18)	2,946 (116)	457 (18)	2	0.1	330 (48)	400 (58)	33 (4.8)	500 (112)
3CLH18	DC	457 (18)	457 (18)	2,946 (116)	457 (18)	3	0.1	330 (48)	400 (58)	25.6 (3.7)	500 (112)
No. 2	DC	457 (18)	457 (18)	2,946 (116)	305 (12)	2.5	0.17	434 (63)	476 (69)	21.1 (3.1)	2,650 (596)
N18M	DC	300 (11.8)	300 (11.8)	900 (35.4)	100 (3.9)	2.7	0.19	380 (55)	375 (54)	26.5 (3.8)	429 (96)
TP-30	SC	400 (15.7)	400 (15.7)	2,700 (106)	50 (2)	1.49	0.28	374 (54)	363 (53)	31.1 (4.5)	160 (36)
No. 1	DC	200 (7.9)	400 (15.7)	1,000 (39)	128 (5)	2.53	1	360 (52)	345 (50)	45 (6.5)	0

Note: DC=double curvature, or with two fixed ends; SC=single curvature, or cantilever; b=width of the section; h=depth of the section; L_{in}=length of the column from the inflection point to the end section; S_h=hoop spacing; ρ_g=longitudinal reinforcement ratio; ρ_w=transverse reinforcement ratio; f_{yx}=longitudinal reinforcement yield stress; f_{yy}=transverse reinforcement yield stress; f'_c=concrete compression strength; and P=axial load.

ignored. For a few special cases, such as short columns with low transverse ratios, the shear strain component should be considered in the analysis.

Case II

When strain in the transverse reinforcement is greater than yield strain, $\varepsilon_y \geq \varepsilon_{yy}$. In this case, $f_{sy}=f_{syy}$, where f_{syy}=yield stress of the transverse reinforcement.

Hence

$$\varepsilon_1 = \frac{(\varepsilon_x - \varepsilon_2)(f_{c1} - f_{cx})}{(f_{c1} + \rho_{sy} f_{syy})} + \varepsilon_x \tag{23}$$

where f_{c1} is determined based on the same approach as described in Case I.

Shear Stress Limitation at Cracks

The MCFT limits the maximum shear stress transferred by aggregate interlock across a crack surface using the following formulation based on the Walraven equation:

$$\tau_i \leq \frac{0.18\sqrt{f'_c}}{0.31 + \dfrac{24w}{a_g + 16}} (\text{MPa, mm}) \tag{24}$$

where $w=s_\theta \varepsilon_1$ and

$$s_\theta = \frac{1}{\dfrac{\sin\theta}{s_x} + \dfrac{\cos\theta}{s_y}}$$

and where s_x and s_y=average crack spacings in the x and y directions, respectively.

Equilibrium in the y direction, at the crack, requires that

$$f_{sycr} = (f_y + \tau \tan\theta - \tau_i \tan\theta)/\rho_{sy} \tag{25}$$

where f_{sycr}=transverse reinforcement stress at the crack; and f_y=clamping stress; which is zero. Hence for $f_{sycr}=f_{syy}$

$$\tau_{max} \leq \tau_i + f_{syy}\rho_{sy} \cot\theta \tag{26}$$

In the USFM, the shear stress on the section must not exceed the value obtained from Eq. (26). For the column in Fig. 6, it is

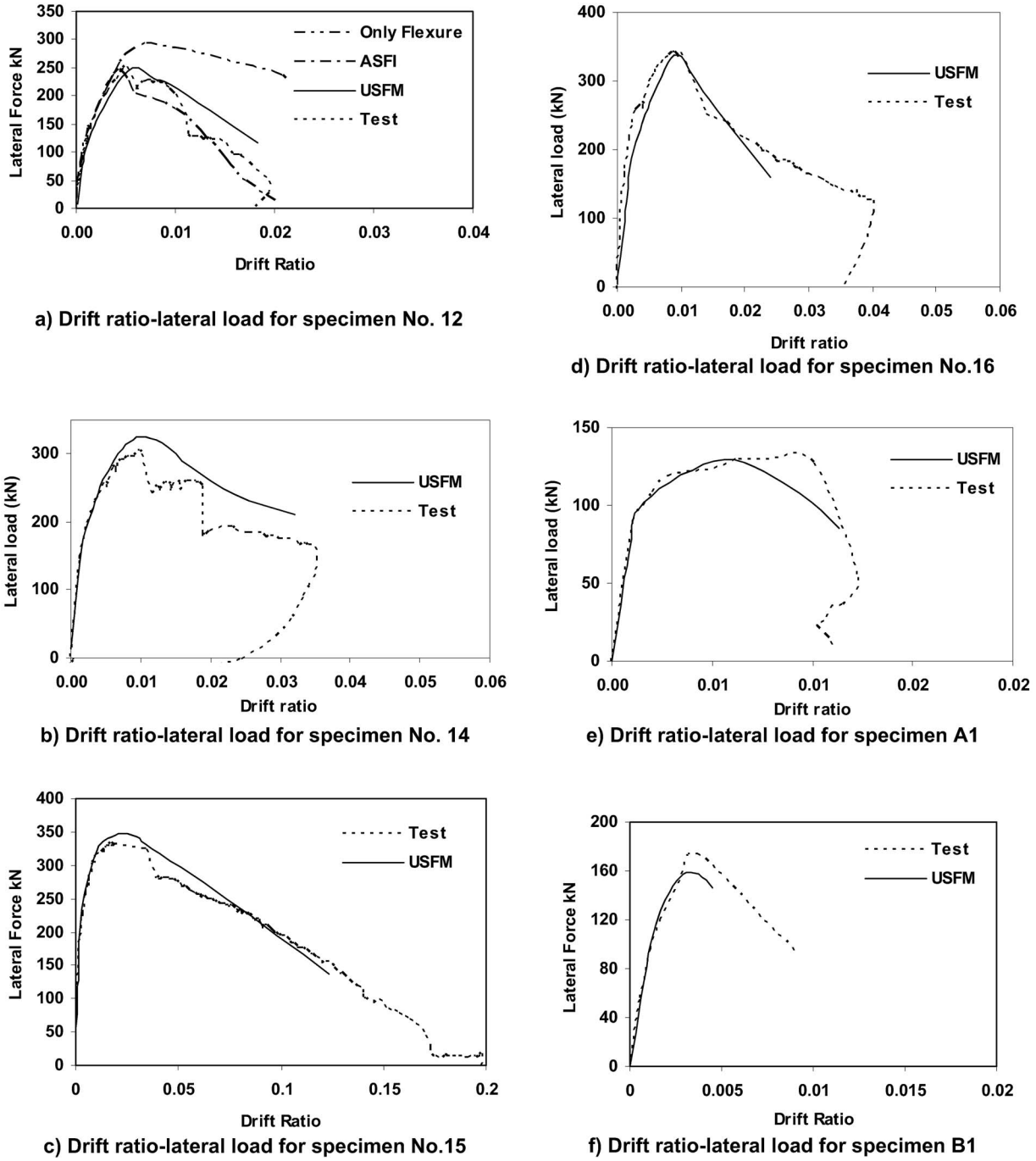

Fig. 7. Comparison of experimental and analytical results

$$\frac{M}{\text{bhL}_{\text{in}}} \leq \tau_i + f_{syy}\rho_{sy}\cot\theta \tag{27}$$

where M = bottom fixed end moment of the column obtained from the section analysis.

Analysis Procedure

Although analytical process of the USFM is basically similar to that of the ASFI method, it is much simpler due to the reduced analytical treatment given to the shear element made by eliminating the complex matrix analysis algorithm required for the full shear model.

Hence, the steps in an analysis performed according to the USFM method, for a given curvature (ϕ) and axial strain (ε_{xi}), are as follows:

1. Apply the section analysis procedure for two adjacent sections (at least one section at the section with maximum moment and one section at the inflection point, where moment is zero, i.e., Sections A and B in Fig 5, and determine the average centroidal strain and concrete principal compression strain between the two sections using Eqs. (5) and (9), respectively.

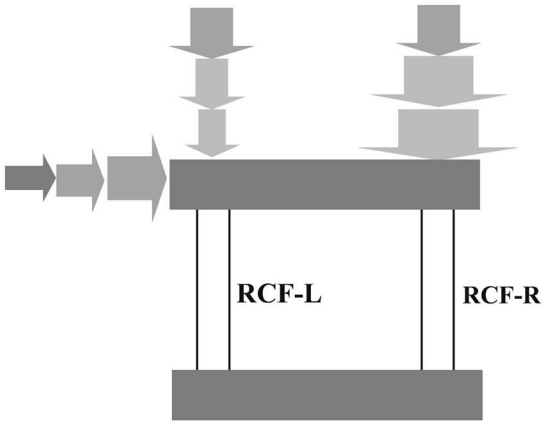

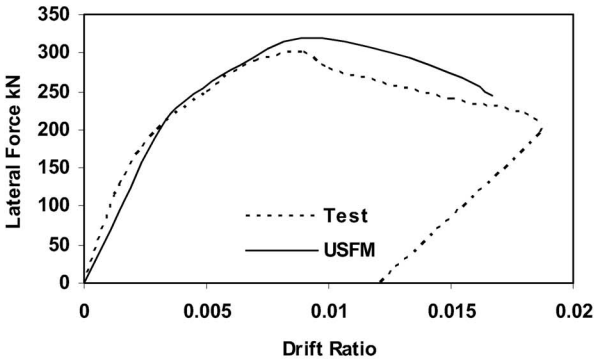

i) Drift ratio-lateral load for specimen No. 2

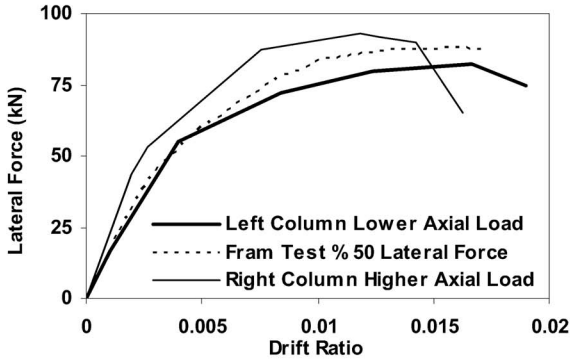

g) Drift ratio-lateral load for specimen RCF

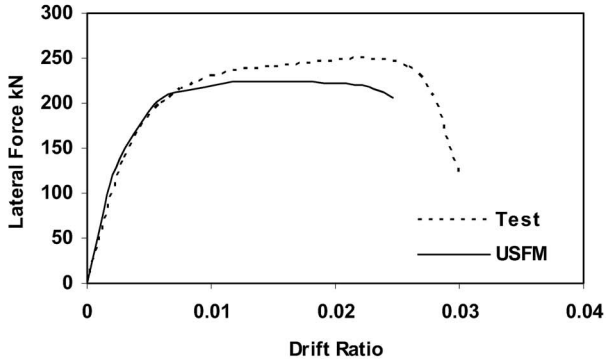

j) Drift ratio-lateral load for specimen 2CLH18

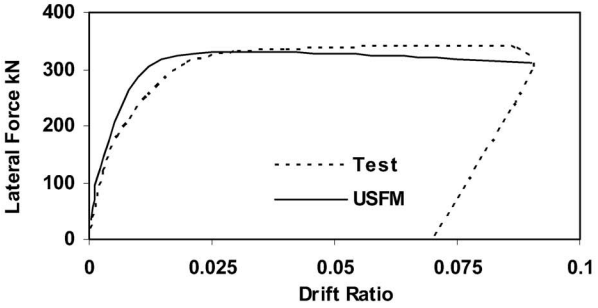

h) Drift ratio-lateral load for specimen U6

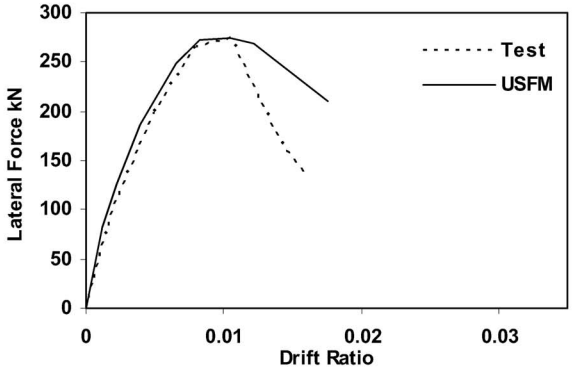

k) Drift ratio-lateral load for specimen 3CLH18

Fig. 7. (*Continued*).

2. Determine the average concrete principal tensile strain ε_1 using Eqs. (18) and (15), assuming an initial value of $0.56f'_t$ for f_{c1}.
3. If the transverse reinforcement has yielded, apply Eq. (23) to determine the average concrete principal tensile strain ε_1; otherwise, go to step 4.
4. Calculate the compression softening factor using Eq. (4) and determine the concrete compression stress of the stress block, multiplied by the compression softening factor.
5. Obtain the moment and shear force, as well as the centroidal strain at the sections, by section analysis.
6. Check for maximum shear stress on crack using Eq. (27).
7. Obtain the total lateral drift ratio and the axial strain using Eq. (1*a*) where $\gamma_s=[2(\varepsilon_x-\varepsilon_2)]/(\tan\theta)$ and $\gamma_f=\delta/L_{in}=1/L_{in}\int_0^{Lin}x\phi dx$ where ϕ=curvature at distance x, corresponding to the inflection point, of the column. In the next increment of the section analysis, for more accuracy, the axial strain may be determined using Eq. (22). In addition, given the value of ε_1 determined, f_{c1} can be found from Eq. (19).

Lateral deformation due to pullout,γ_{pul} in Fig. 4, or slip of steel bars under tension stress at the end section, adjacent to the section with larger thickness, can be determined based on the method described in the ASFI approach, and added in Eq. (1*a*). In

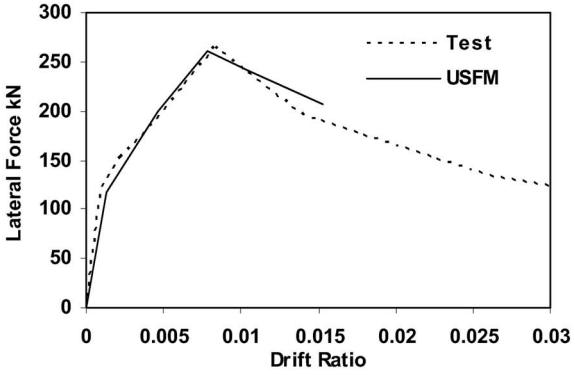

l) Drift ratio-lateral load for specimen N18M

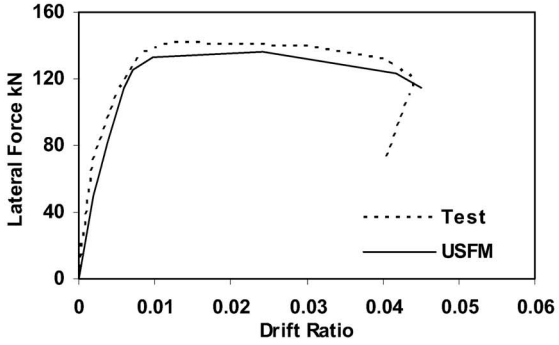

m) Drift ratio-lateral load for specimen TP-30

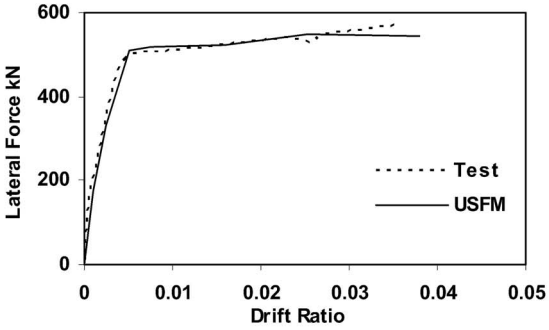

n) Drift ratio-lateral load for specimen No.1

Fig. 7. (*Continued*).

the analysis of specimens in Table 1, pullout deformation is included in the load-deformation response of the specimens.

Model Verification

To verify the applicability and accuracy of the USFM approach for reinforced concrete columns and beams, specimens with various performance characteristics were selected and evaluated using the developed method. The geometry and material properties for all the specimens considered are listed in Table 1. Fig. 7 illustrates comparison between experimental and theoretical results for all 14 specimens. For the sake of comparison, only the envelope curves of the specimens under cyclic loads are shown.

Specimen Nos. 12, 14, 15, 16, RCF-L, and RCF-R were loaded, laterally, under static cyclic unidirectional reverse load. For the first four specimens, the axial loads were identical and constant. Specimens RCF-L and RCF-R were two columns of a one-bay frame with rigid top and bottom stubs, under varying axial loads related to the applied lateral load. The column specimens were scaled to 1/3 of actual columns, representing columns located in the midframe of the first floor of a building with moderate height.

Comparing experimental results from the first four columns to the test outcomes of the columns with different hysteretic loading patterns indicated no significant effects on column response due to the different lateral loading patterns (Ousalem et al. 2003). Therefore, for the analysis by the USFM method, which is based

on a monotonic loading pattern, the effects of hysteretic loading pattern were neglected for these specimens.

Column Nos. 12, 14, and 15 had almost identical characteristics except for lateral reinforcement ratios. Column No. 12 had the lowest lateral steel ratio and is expected to fail in shear. However, specimen No. 15 was designed to have a flexural response given its high transverse reinforcement ratio. Column No. 14 is expected to perform between that of the two previous columns with a flexural-shear failure. Column specimen No. 16, being shorter compared to the other three columns, is expected to fail in shear-compression mode. Both ends of the columns were considered as moment resistant connections with zero rotation.

Considering the symmetric conditions of the specimens, the two sections required for USFM analysis were chosen as one at the inflection point and one at an end section. Displacement-based analysis was implemented according to the new analytical approach described. As a result, the drift ratio-lateral load responses for the columns were estimated and compared to the test data. As shown in Fig. 7, consistent correlations were obtained. Furthermore, to assess the efficiency of the USFM compare to the traditional section analysis and the original ASFI method, analytical results were obtained for specimen No. 12 also by the ASFI method and a section analysis, as illustrated in Fig. 7(a). The results clearly indicate the benefit of using the USFM over the traditional section analysis—only flexure—without sacrificing the accuracy of the ASFI approach.

In the analysis using USFM, in order to consider buckling or slip of the compression bars, the compression strengths of the longitudinal bars were assumed to start to degrade when the stress within the unconfined-cover concrete reached about 30% of the maximum concrete strength. They were then linearly decreased according to the slope of the postpeak confined-core concrete compression stiffness.

Column specimens RCF-L and RCF-R were loaded in a one-bay frame system (Mostafaei 2006). Considering lateral loading in the positive direction, as shown in Fig. 7(g), column RCF-L was subjected to a decreasing axial load and column RCF-R was subjected to an increasing axial load. Therefore, different responses are expected for the two columns. Analytical and experimental results for the individual columns and the frame are compared and depicted in Fig. 7(g), leading to reasonable agreement. To apply the USFM method for further response evaluation of shear critical columns, two column specimens A1 and B1 (Koizumi 2000) were selected. Both specimens had very low transverse reinforcement ratios with a considerably high axial load ratio. Employing the analysis described, acceptable correlations between analysis and test response were achieved for both columns as shown in Figs. 7(e and f).

Specimen U6 (Saatcioglu and Ozcebe 1989), among all the specimens, had the largest ultimate drift ratio of about 10%. To assess the applicability of the simplified USFM method considering the size effect, three full-scale columns, No. 2CLH18, No. 3CLH18 (Lynn et al. 1996), and No. 2 (Sezen 2000) were selected, given their totally different performances. Specimen No. 2CLH18 had a flexure-dominant behavior while No. 3CLH18 performed as a shear-critical column. Specimen No. 2 had the greatest applied axial load ratio of about 60%, compared to the other specimens. Specimen N18M (Nakamura and Yoshimura 2002) is another shear-critical column with a very low transverse reinforcement ratio, but with the same geometry as that of the first three columns. Again, the correlation between calculated and observed responses is strong, as seen in Figs. 7(h–l).

A reinforced concrete column of a bridge, TP-30 (Nagaya and Kawashima 2002), was also analyzed; this column had a flexure-dominant response. Finally, in order to verify the proposed model for beams, a specimen with zero axial load, specimen No. 1 (Umemura et al. 1977) was modeled by the simplified USFM method. The results for these two specimens are compared with the test data in Figs. 7(m and n). A high degree of accuracy in the calculated load-deformation responses was achieved for these specimens as well.

Conclusions

A new simple displacement-based evaluation method for reinforced concrete columns and beams is presented based on a modification of traditional sectional analysis procedures. The effects of shear are taken into account by imposing a concrete strength degradation within the stress block calculations. Both the axial strain and principal compression strain arising from the shear mechanism are derived and included with the strains of the section analysis. A simple formulation was derived and is employed to determine the concrete principal tensile strain as well as compression softening factor; the simplifications introduced allow the analyses to be reduced to a uniaxial problem. The proposed displacement-based evaluation approach was verified by performing analyses for a number of diverse test specimens, and comparing calculated to observed responses. Consistently strong correlations were attained between the analytical results and experimental outcomes.

References

Koizumi, H. (2000). "A study on a new method of sheet strengthening to prevent axial collapse of RC columns during earthquakes." MS thesis, Faculty of Engineering, Architrave Dept., Univ. of Tokyo, Tokyo (in Japanese).

Lynn, A. C., Moehle, J. P., Mahin, S. A., and Holmes, W. T. (1996). "Seismic evaluation of existing reinforced concrete building columns." *Earthquake Spectra*, 12(4), 715–739.

Mostafaei, H. (2006). "Axial-shear-flexure interaction approach for displacement-based evaluation of reinforced concrete elements." Ph.D. thesis, Faculty of Engineering, Architrave Dept., Univ. of Tokyo, Tokyo.

Mostafaei, H., and Kabeyasawa, T. (2005). "A simple approach for displacement-based assessment of RC columns." *Proc. 1st NEES/E-Defense Workshop on Collapse Simulation of Reinforced Concrete Building Structure*, Univ. of California Berkeley, Earthquake Engineering Reseach Center, PEER 2005/10, 47–63.

Mostafaei, H., and Kabeyasawa, T. (2007). "Axial-shear-flexure interaction approach for reinforced concrete columns." *ACI Struct. J.*, 104(2), 218–226.

Nagaya, K., and Kawashima, K. (2002). "Effect of aspect ratio and longitudinal reinforcement diameter on seismic performance of reinforced concrete bridge columns." *Rep. No. TIT/EERG 01*, Tokyo Institute of Technology, Tokyo.

Nakamura, T., and Yoshimura, M. (2002). "Gravity collapse of reinforced concrete columns with brittle failure modes." *J. Asian Architecture and Building Engineering*, 1(1), 21–27.

Okamura, H., Maekawa, K. (1991). "Nonlinear analysis and constitutive models of reinforced concrete." *Gihodo Shuppan Co., Ltd.*, Tokyo.

Ousalem, H., Kabeyasawa, T., Tasai, A., and Iwamoto, J. (2003). "Effect of hysteretic reversals on lateral and axial capacities of reinforced concrete columns." *Proc., Japan Concrete Institute*, 25(2), 367–372.

Saatcioglu, M., and Ozcebe, G. (1989). "Response of reinforced concrete columns to simulated seismic loading." *ACI Struct. J.*, 86(1), 3–12.
Sezen, H. (2000). "Evaluation and testing of existing reinforced concrete columns." *CE 299 Rep.*, Dept. of Civil and Environmental Engineering, UC Berkeley, Berkeley, Calif.
Umemura, H., Aoyama, H., and Noguchi, H. (1977). "Experimental studies on reinforced concrete members and composite steel and reinforced concrete members." Faculty of Engineering, Dept. of Architecture, Univ. of Tokyo, Vol. 2, 113–130.
Vecchio, F. J., and Collins, M. P. (1986). "The modified compression field theory for reinforced concrete elements subjected to shear." *ACI J.*, 83(2), 219–231.